



OPEN

SUBJECT AREAS:

GENE THERAPY

GENE DELIVERY

Received
17 July 2013Accepted
9 January 2014Published
24 January 2014

Correspondence and
requests for materials
should be addressed to
Y.N. (negishi@toyaku.
ac.jp)

Systemic delivery of miR-126 by miRNA-loaded Bubble liposomes for the treatment of hindlimb ischemia

Yoko Endo-Takahashi¹, Yoichi Negishi¹, Arisa Nakamura¹, Saori Ukai¹, Kotomi Ooaki¹, Yusuke Oda², Katsutoshi Sugimoto³, Fuminori Moriyasu³, Norio Takagi⁴, Ryo Suzuki², Kazuo Maruyama² & Yukihiro Aramaki¹

¹Department of Drug Delivery and Molecular Biopharmaceutics, School of Pharmacy, Tokyo University of Pharmacy and Life Sciences, 1432-1 Horinouchi, Hachioji, Tokyo 192-0392, Japan, ²Laboratory of Drug and Gene Delivery Research, Faculty of Pharma-Sciences, Teikyo University, 2-11-1 Kaga, Itabashi-ku, Tokyo 173-8605, Japan, ³Department of Gastroenterology and Hepatology, Tokyo Medical University, 6-7-1 Nishishinjuku, Shinjuku-ku, Tokyo 160-0023, Japan, ⁴Department of Applied Biochemistry, School of Pharmacy, Tokyo University of Pharmacy and Life Sciences, 1432-1 Horinouchi, Hachioji, Tokyo 192-0392, Japan.

Currently, micro RNA (miRNA) is considered an attractive target for therapeutic intervention. A significant obstacle to the miRNA-based treatments is the efficient delivery of miRNA to the target tissue. We have developed polyethylene glycol-modified liposomes (Bubble liposomes (BLs)) that entrap ultrasound (US) contrast gas and can serve as both plasmid DNA (pDNA) or small interfering RNA (siRNA) carriers and US contrast agents. In this study, we investigated the usability of miRNA-loaded BLs (mi-BLs) using a hindlimb ischemia model and miR-126. It has been reported that miR-126 promotes angiogenesis via the inhibition of negative regulators of VEGF signaling. We demonstrated that mi-BLs could be detected using diagnostic US and that mi-BLs with therapeutic US could deliver miR-126 to an ischemic hindlimb, leading to the induction of angiogenic factors and the improvement of blood flow. These results suggest that combining mi-BLs with US may be useful for US imaging and miRNA delivery.

Micro RNA (miRNA) are endogenous non-coding small RNA that negatively regulate gene expression at the post-transcriptional level in various processes. Using computer-based predictions, numerous miRNAs have been discovered, and many have been proven to affect cell functions in most tissues. miRNAs are considered to play a crucial role in proliferation, differentiation, development, and survival. It is becoming increasingly apparent that the aberrant expression of miRNAs is causally related to a variety of disease states. The apparent roles of miRNAs in disease have led to increasing interest in miRNA regulation as a therapeutic and diagnostic approach.

miR-126 is encoded by intron 7 of the *egfl7* gene and is highly expressed in endothelial cells¹. Knock-out studies in zebrafish and mice have suggested a major role for miR-126 in angiogenesis and vascular integrity, which was mediated by the repression of inhibitors of VEGF-induced signaling in endothelial cells^{1,2}. Furthermore, previous research using a mouse ischemic hindlimb model and an antagomir specifically targeting miR-126 has demonstrated that the functional activity of miR-126 is required for an ischemia-induced angiogenic response³. These findings suggest that miR-126 may be an important target for proangiogenic therapy. However, as for many other therapeutic approaches, the biggest hurdle in modifying miRNA expression might be the targeted delivery of oligonucleotides. Few have reported nonviral systemic delivery of miRNA, although a delivery system in the blood vessels could be useful for the delivery of miR-126 into endothelial cells.

We previously developed “Bubble liposomes” (BLs). These liposomes are polyethylene glycol (PEG)-modified liposomes that contain echo-contrast gas, which can function as a novel plasmid DNA (pDNA) and small interfering RNA (siRNA) delivery tool when used with ultrasound (US) exposure *in vitro* and *in vivo*^{4–8}. Furthermore, to increase the efficiency of nucleic acid delivery via systemic administration, we prepared pDNA-loaded BLs (p-BLs) and siRNA-loaded BLs (si-BLs) using 1,2-dioleoyl-3-trimethylammonium-propane (DOTAP), a cationic lipid often used for gene delivery^{9,10}. These types of BLs improved the stability of nucleic acids in the presence of serum so that the effects of nucleic acid delivery could be observed. Additionally, by

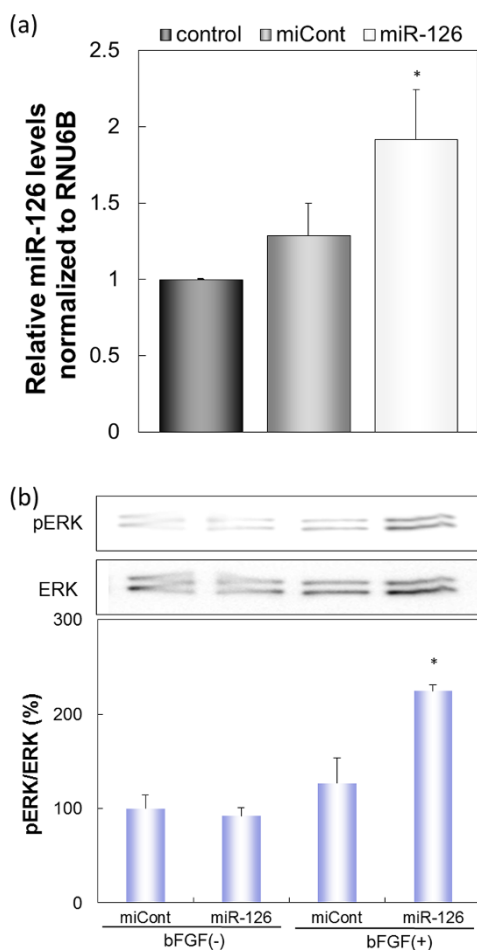


Figure 1 | The effects of transfecting HUVECs with miR-126. (a) miR-126 levels in HUVECs transfected with miRNA (100 nM) using BLs (60 μ g) and US at three days post-transfection. control: the non-transfected group; miCont: the group transfected with control miRNA; miR-126: the group transfected with miR-126. (b) The activation of VEGF signaling with or without bFGF by transfection with miR-126. To estimate ERK activation, the levels of phosphorylated ERK (pERK) were analyzed by western blotting. Quantification of band intensity was performed with ImageJ software. Full scans of the blots are available in Supplementary Information, Figure S1. * indicates $P < 0.05$ using a one-way ANOVA with Tukey's post-hoc test. All data represent the mean \pm SD ($n = 3-4$).

changing the lipid composition of the p-BLs, not only the gene delivery effects but also the US imaging effects were improved, and the p-BLs were shown to be an effective therapeutic tool in a hindlimb ischemia mouse model¹¹.

In this study, we initially prepared miRNA-loaded BLs (mi-BLs) and evaluated their physical properties, miRNA loading ratio, and usability as a US contrast agent. Furthermore, we investigated the therapeutic effect of miR-126 in hindlimb ischemia by systemic administration of mi-BLs coupled with US exposure.

Results

We initially transfected HUVECs with miR-126 via BLs and US and investigated the effects on the angiogenic signaling pathway. As a result, the amount of miR-126 in the HUVECs transfected with miR-126 was significantly higher than in control cells and HUVECs transfected with control miRNA (Fig. 1a). Furthermore, the activation of ERK phosphorylation in the presence of bFGF was enhanced in the miR-126-transfected group, whereas activation was not observed in the control miRNA-transfected group (Fig. 1b). These results suggest

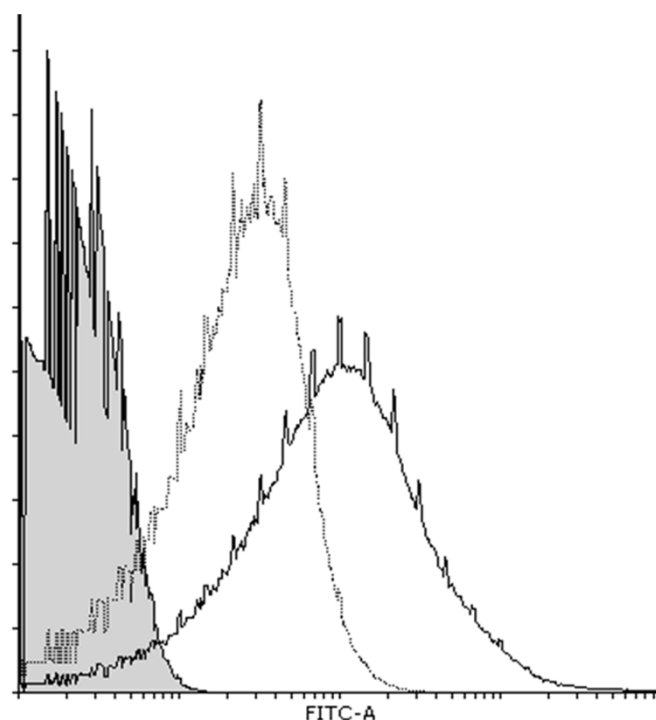


Figure 2 | The interaction of miRNA and BLs. The interaction was examined by analyzing a solution of mi-BLs containing FITC-miRNA (50 pmol) and BLs (60 μ g) with a FACSCanto. Gray area: BLs only; solid line: mi-BLs containing cationic lipid; dotted line: miRNA and BLs not containing cationic lipid.

that an increased intracellular miR-126 concentration can activate the angiogenic signaling pathway in HUVECs and that the physical energy of BLs and US had no effect on the signaling pathway.

Before *in vivo* transfection experiments, we examined the interaction between miRNA and BLs containing the cationic lipid DSDAP, which was previously reported to be an effective cationic lipid for the preparation of p-BLs¹¹. We found that the amount of miRNA bound to the BLs increased in the presence of cationic lipid (Fig. 2). The miRNA loading ratio of the BLs containing DSDAP was approximately 80%, and there were no differences in the ratio between miR-126 and control miRNA. BLs containing DSDAP enable to carry about 1340 miRNA molecules per BL. There were no apparent changes in size between the BLs and the mi-BLs, and the zeta potential of the BLs containing cationic lipid decreased with miRNA loading (Table 1). It has been reported that cationic liposomes often cause the agglutination of erythrocytes and high levels of hemolysis due to the interaction of the lipid component with the erythrocyte membrane^{12,13}. We assessed the interaction of BLs with erythrocytes using an *in vitro* hemolysis assay. The BLs showed negligible hemolysis after a 4-hr incubation (Fig. 3). These results suggest that BLs have little effect on erythrocytes.

To evaluate the usability of mi-BLs as a miR-126 delivery tool via intravascular injection, we used a hindlimb ischemia mouse model at 10 days post-ligation. We first confirmed whether mi-BLs could access the ischemic hindlimb using diagnostic US equipment. As

Table 1 | Size and zeta potential of BLs and mi-BLs

	Mean Size (nm)		Zeta Potential (mV)	
	BLs	mi-BLs	BLs	mi-BLs
Cation(-)	589.3 \pm 66.4	540.2 \pm 69.4	-3.67 \pm 1.09	-4.22 \pm 1.08
Cation(+)	430.2 \pm 52.8	490.7 \pm 65.6	8.17 \pm 0.74	5.00 \pm 1.69

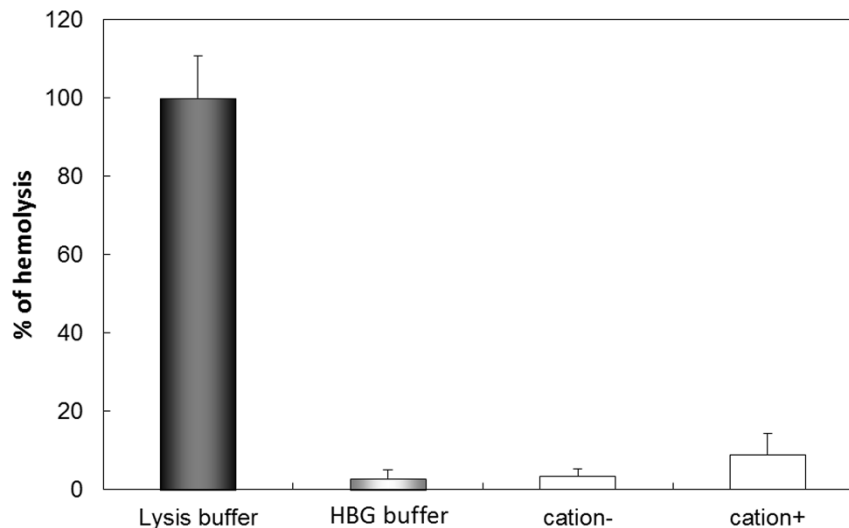


Figure 3 | Hemolysis test of BLs containing cationic lipid. Red blood cell suspensions were incubated with BLs or buffer for 4 hr at 37°C.

shown in Figure 4, the delivery of mi-BLs to the ischemic hindlimb was observed at the same level as the solution of miRNA and BLs not containing cationic lipid.

To determine the efficacy of the therapeutic effect, we treated an ischemic hindlimb with miR-126 using mi-BLs and US on post-ligation days 10 and 12. Two days after the second injection, the amount of miR-126 in the group treated with miR-126 by mi-BLs containing cationic lipid was significantly higher than in the group treated with control miRNA (Fig. 5a). In contrast, there was no significant difference between the two groups treated with BLs not containing cationic lipid. The level of miR-126 persisted for at least seven days. Furthermore, the mRNA levels of various angiogenic factors significantly increased with increasing miR-126 levels (Fig. 5b, 5c). On day 14, no significant recovery of blood flow was observed. On day 19, however, the blood flow rate in the group treated with miR-126 via mi-BLs significantly improved compared with the control group, which was treated with saline, BLs not containing cationic lipid, or control miRNA (Fig. 5d). These results suggest that the combination of mi-BLs and US exposure could be a useful systemic miRNA delivery system and that miR-126 could be effective for angiogenic gene therapy.

Discussion

It is widely recognized that modulation of miRNA expression or action contributes to the development of a numerous human diseases. Recently, miRNA was identified as an attractive target for therapeutic intervention. The main bottleneck for the development of miRNA-based treatments is the efficient delivery of a therapeutic RNA to its target tissue.

We previously developed nanosized p-BLs using cationic lipids and demonstrated that the loading of pDNA onto BLs improved the efficiency of delivery via systemic administration. We also

showed that BLs containing DSDAP were effective not only as a gene delivery tool but also as a US contrast agent. Moreover, the delivery of pDNA encoding the bFGF gene by p-BLs and US into an ischemic hindlimb led to an improvement in blood flow^{9,11}. Similar effects could be achieved by combining US and a local injection of pDNA and either commercial microbubbles or our BLs into muscle^{14,15}. However, a local injection could limit the region of gene transfection to the myocytes and partial capillaries surrounding the injection site. Angiogenic gene therapy by systemic injection could be hypothesized to increase the accessibility of deep tissues and vascular endothelial cells to genes. Therefore, an injection of nucleic acid-loaded BLs via systemic injection could be effective therapeutic method for ischemic diseases.

Recently, it has been reported that pDNA bound to cationic lipid-shelled microbubbles via electrostatic charge coupling led to an increase in gene transfection *in vitro* and *in vivo*^{16–18}. However, the microbubbles used in these reports had a size of 1–5 μm . These microbubbles have difficulty penetrating deep into tissues. Our nanosized BLs are potentially superior carriers for extensive delivery into tissues. Our nanosized BLs are potentially superior carriers for extensive delivery into tissues. Not only the size but also the number of BLs could have an effect on US-induced cavitation, which is the process of bubble oscillation and collapse. Cavitation has been proposed to temporarily improve the permeability of cell membranes, enabling the transport of extracellular molecules into viable cells^{19,20}. We were able to check the mean size of the BLs, but it was difficult to accurately measure the number of BLs because of their small size. In this study, we estimated the particle number according to a previous report²¹. However, we should obtain accurate information and investigate the differences in the induced cavitation depending on the number of BLs in the future.

We also confirmed the delivery of FITC-miRNA into the ischemic hindlimb treated with the combination of mi-BLs and US. As a result,

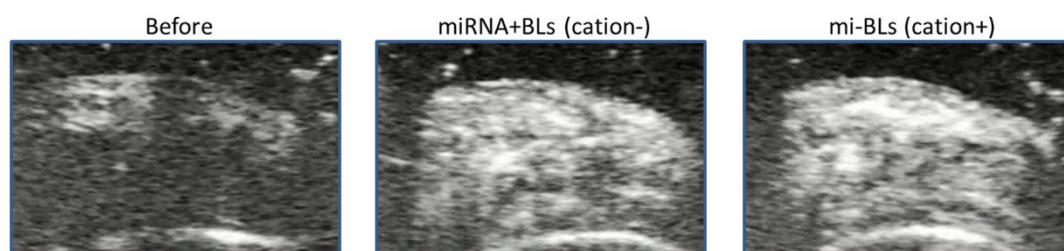


Figure 4 | Ultrasonographic images of ischemic hindlimbs 30 sec after injection with mi-BLs (1 mg/mL, 200 μL).

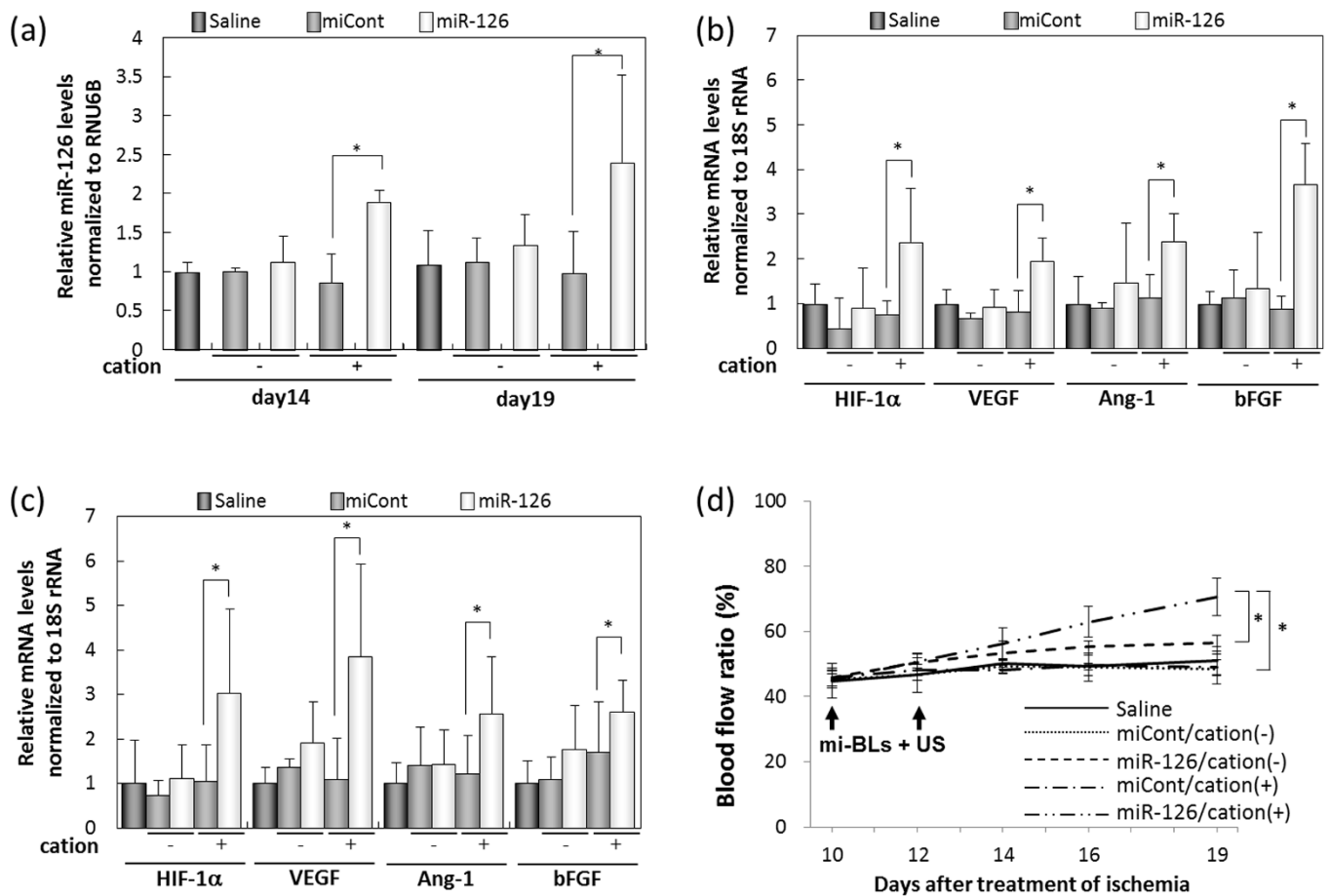


Figure 5 | The therapeutic effects of miR-126 transfer by mi-BLs and US exposure on mice with hindlimb ischemia. Ten days after femoral artery ligation, mice were treated with mi-BLs and US. The treatment was administered via tail vein injection twice daily every two days to mice with hindlimb ischemia. We injected a solution of miRNA (40 μ g of miCont or miR-126) and BLs (200 μ g). (a) miR-126 levels in the ischemic hindlimb after transfection. (b), (c) The effect of miR-126 transfer by mi-BLs and US on mRNA expression for angiogenic genes. Two (b) or seven (c) days after the second transfection, RNA was isolated from the thigh muscle and analyzed using real-time PCR. (d) The effect of miR-126 transfer using mi-BLs and US on the recovery of blood flow. After the second transfection, blood flow was measured using a laser Doppler blood flow meter. All data are reported as the mean \pm SD ($n = 4-6$). * indicates $P < 0.05$ using a one-way ANOVA with Tukey's post-hoc test.

FITC-miRNA could be observed in the ischemic muscle that was exposed to US just after US exposure (data not shown). The delivery effect was observed in the tissue exposed to US, but no FITC-miRNA was observed in the contralateral leg that was not exposed to US. This result is consistent with the findings of our previous reports on pDNA delivery¹¹. These results suggest that miRNA delivery by US and mi-BLs should provide specific transfection in the US-exposed area within a fairly short timeframe. Furthermore, FITC-miRNA was mostly observed in the intercellular space of the myofibers, including the endothelial cells, and partly observed in muscle cells. These results indicate that the miRNA was delivered to the ischemic tissues through blood vessels and extravasated with US exposure. However, the type of cells that contributed to angiogenesis along with miR-126 transfected by our method was unclear. Future experiments should be conducted to obtain this information.

miR-126 has been suggested to play a critical role in vascular development. Moreover, following myocardial infarction, miR-126-knockout mice showed impaired vascular growth in the infarct border zone¹. Previous research using a mouse ischemic hindlimb model has also demonstrated that the functional activity of miR-126 is required for an ischemia-induced angiogenic response³. However, there is little information about miR-126 replacement therapy. In the current study, at day 10 post-ligation, miR-126 levels in the ischemic left hindlimb were significantly lower than in the normal right

hindlimb (data not shown). This finding might be due to a reduction in endothelial cells due to the excision of vessels. We assumed that the transfection of miR-126 into an ischemic hindlimb could be an effective therapeutic modality. We observed the activation of ERK following miR-126 transfection with BLs and US. miR-126 represses the expression of SPRED1 and PI3KR2, which negatively regulate VEGF signaling via the ERK and AKT pathways, respectively^{1,2}. Our result was consistent with the findings of previous reports. It has been reported that VEGF promoted angiogenesis through the phosphorylation of ERK and AKT in a mouse ischemic hindlimb²². The therapeutic effects demonstrated in the study may be due to a similar mechanism.

Recently, several studies showed that gene therapy involving multiple angiogenic factors or a combination of gene therapy and cell-based therapy could be useful in ischemic diseases^{23,24}. On average, miRNA can regulate several hundred transcripts whose effector molecules function at various sites within cellular pathways and networks. Thus, miRNAs can instantly switch between cellular programs and are therefore often viewed as master regulators of the human genome. miRNAs with an influence on several factors could be an effective tool for angiogenic therapy.

The relationship between miR-126 and various diseases was recently reported. The upregulation of miR-126 levels by retroviral infection in primary breast cancer cells suppressed overall tumor



growth and metastasis to the bone and lung in nude mice²⁵. The downregulation of miR-126 induces angiogenesis and lymph angiogenesis by activation of VEGF-A in oral cancer²⁶. Mesenchymal stem cells (MSCs) overexpressing miR-126 enhanced ischemic angiogenesis via the AKT/ERK-related pathway²⁷. Diabetes led to decreased miR-126 levels, and the proangiogenic effects of CD34(+)-peripheral blood mononuclear cells (PBMNCs) could be restored by miR-126 transfection²⁸. These reports showed that the effects of miR-126 on angiogenesis might substantially differ between diverse cell types and pathophysiological settings. Moreover, the effects of miR-126 on cells are likely not fully understood. The overexpression of miR-126 must be carefully considered because there is no direct evidence regarding excessive introduction of miR-126. Therefore the targeted delivery of miRNA is crucial to miRNA therapy. It would be easy to modify liposomes to add a targeting function. We have successfully developed targeted BLs modified with peptide²⁹. With a targeting ability, the mi-BLs developed in this study could lead to a useful therapeutic strategy based on miRNA. Furthermore, BLs could also be effective tools for US diagnosis. The term theranostics, which is derived from “diagnostics” and “therapeutics,” refers to a treatment strategy that combines a diagnostic test and a specific therapy based on the test results. A vascular lesion could be visualized using diagnostic US and targeted BLs and could be efficiently treated with therapeutic US and mi-BLs. Recently, a device with US core wire and a multilumen infusion catheter was developed and has already gained approval from the Food and Drug Administration. The catheter could improve the effectiveness of drug delivery, such as the delivery of thrombolytic agents, with the application of US³⁰. The combination of mi-BLs and a similar catheter-type US could also be useful because miRNA and BLs need to be efficiently delivered from the injection site to the exposure site. Moreover, mi-BLs may have widespread applications as delivery tools for other type of miRNAs or antagomirs. Thus, the combination of mi-BLs and US has strong potential to become a theranostic agent and to have beneficial clinical applications in various diseases.

In this study, we showed that BLs containing DSDAP were efficiently loaded with miRNA and pDNA. Furthermore, we demonstrated that the mi-BLs reached an ischemic site after intravascular injection, were detected by diagnostic US, and delivered miR-126 following therapeutic US. The delivery of miR-126 led to the induction of angiogenic factors and improved blood flow. This is the first report showing the usability of miR-126 replacement therapy for angiogenic treatment by combining US and a bubble formulation in a hindlimb ischemia model. These results suggest that the combination of mi-BLs and US exposure may be useful for US imaging and for the delivery of miRNA to tissues or organs via systemic administration. This combination may serve as a diagnostic and therapeutic system.

Methods

Preparation of liposomes and BLs. To prepare liposomes for BLs that do not contain cationic lipid, 1,2-distearoyl-sn-glycero-phosphatidylcholine (DSPC) and 1,2-distearoylphosphatidylethanolamine-methoxy-polyethylene glycol (PEG₂₀₀₀) were mixed at a molar ratio of 94 : 6. Both lipids were purchased from NOF Corporation (Tokyo, Japan). For BLs containing cationic lipid, 1,2-distearoyl-3-dimethylammonium-propane (DSDAP) from Avanti Polar Lipids (Alabaster, AL) was used. Liposomes with various lipid compositions were prepared using the reverse phase evaporation method as described previously⁷. Briefly, DSPC, cationic lipid, and PEG₂₀₀₀ were mixed at a molar ratio of 64 : 30 : 6 and dissolved in 1 : 1 (v/v) chloroform/diisopropylether. HEPES-buffered glucose (HBG: 5% glucose, 10 mM HEPES) was added to the lipid solution, and the mixture was sonicated and then evaporated. The organic solvent was completely removed, and the size of the liposomes was adjusted to less than 200 nm using extrusion equipment and a sizing filter (Nuclepore Track-Etch Membrane, 200-nm pore size; Whatman plc, Kent, UK). After sizing, the liposomes were filter-sterilized using a 0.45-μm syringe filter (Asahi Techno Glass Co., Chiba, Japan).

The liposome concentration was determined using a phosphorus assay. BLs were prepared from liposomes and perfluoropropane gas (Takachiho Chemical Inc. Co. Ltd., Tokyo, Japan). First, 5-mL sterilized vials containing 2 mL of liposome suspension (total lipid concentration: 1 mg/mL) were filled with perfluoropropane gas,

capped, and then pressurized with 7.5 mL of perfluoropropane gas. The vials were placed in a bath sonicator (42 kHz, 100 W; Branson 2510-DTH; Branson Ultrasonics Co., Danbury, CT) for 5 min to form BLs. The zeta potential and mean size of the BLs were determined using a light scattering method with a zeta potential/particle sizer (Nicomp 380ZLS, Santa Barbara, CA). The particle number was estimate using the equation in a previous report²¹. To measure the amount of gases, BLs were analyzed with GC-MS. We used the automatic headspace sampler, HS20 (Shimadzu Co., Kyoto, Japan). The headspace injector was connected with GCMS-QP2010 (Shimadzu Co., Kyoto Japan). The column used for the chromatographic analysis was Rt-Q-BOND (Restek Co., Bellefonte, PA). The amount of perfluoropropane was analyzed by the ion peak area at m/z 69. The ion at m/z 119 and 169 were used for confirmation of the identity of the peak. We calculated that our BL contained around 4.991×10^{-17} L C₃F₈ gas/particle.

Cell cultures. Human umbilical vein endothelial cells (HUVECs) were cultured in Endothelial Cell Growth Medium (Cell Applications Inc., San Diego, CA) supplemented with 10% heat-inactivated fetal bovine serum (FBS; Equitech Bio Inc., Kerrville, TX), 100 U/mL penicillin, and 100 μg/mL streptomycin in a humidified atmosphere containing 5% CO₂ at 37°C.

Transfection of miRNA into cells. The day before transfection, 1×10^4 cells were seeded in the wells of a 48-well plate (Asahi Techno Glass Co., Chiba, Japan). Synthetic miR-126 (hsa-mir-126) and negative-control miRNA (miCont; cel-mir-67) were purchased from BONAC Corporation (Fukuoka, Japan). A mixture of the miRNA (final concentration of 100 nM) and BLs (60 μg (total lipid)) in culture medium containing 10% FBS was added to the cells. The cells were immediately exposed to US (frequency, 2 MHz; duty, 50%; burst rate, 2.0 Hz; intensity, 2.0 W/cm²) for 10 sec using a 6 mm-diameter probe placed in each well and then washed twice with culture medium. A Sonopore 3000 (NEPA GENE, CO., LTD., Chiba, Japan) was used to generate the US.

Three days after transfection, the total RNA was extracted with RNAiso Plus (Takara Bio Inc., Shiga, Japan) according to the manufacturer's instructions. miRNA-specific complementary DNA (cDNA) was synthesized from 100 ng of the total RNA using a TaqMan MicroRNA Reverse Transcription Kit (Life Technologies, Carlsbad, CA) and miRNA-specific RT primers from a TaqMan MicroRNA Assay (Life Technologies). Validation of miR-126 levels was performed using an miRNA-specific probe from a TaqMan MicroRNA Assay and real-time RT-PCR system (ABI PRISM 7000; Life Technologies). For normalization, validation of U6 small nuclear RNA (RNU6B) was performed on cDNA obtained from the same RNA.

For western blotting, two days after transfection, cells were serum-starved in medium containing 0.1% FBS without growth factors overnight and then stimulated with 10 ng/mL bFGF (Pepro Tech Inc., Rocky Hill, NJ) for 15 min. The cells were lysed in lysis buffer (10 mM Tris-HCl, 150 mM NaCl, 1% Triton X-100, 0.1 mM Na₃VO₄, 1 mM PMSF, 5 mM EDTA, 10 mg/mL leupeptin, and 10 mg/mL aprotinin). Samples (5 μg of protein) were separated by 12% SDS-PAGE, and the separated proteins were transferred onto Immobilon-P membranes (Nihon Millipore, Tokyo, Japan). The membranes were blocked with 5% skim milk in Tris-buffered saline containing 0.1% Tween 20. For determination of ERK activation, the membranes were reacted with rabbit anti-p44/42 MAPK mAb or rabbit anti-phospho-p44/42 MAPK mAb (Cell Signaling Technology Inc., Beverly, MA). Specific bands were detected using ImmunoStar LD (Wako), and quantification of the band intensity was performed with ImageJ software.

Preparation of mi-BLs. For the preparation of mi-BLs, adequate amounts of miRNA were added to BLs and gently mixed. FITC-labeled miRNA and flow cytometry were used to examine the interaction between miRNA and BLs. The fluorescence intensity of mi-BLs was analyzed using a FACSCanto (Becton Dickinson, San Jose, CA). To quantify the amount of miRNA loaded onto the BL surfaces, the BLs were centrifuged at 2,000 rpm for 1 min, and the unbound miRNA was removed as previously reported³¹. The BL solution and aqueous solution containing unbound miRNA were then boiled for 5 min to solubilize the BLs and prevent background scattering. The optical density was measured at 260 nm using a spectrophotometer.

Hemolysis assay. Mouse erythrocytes were washed three times at 4°C by centrifugation at 1,000 rpm (Kubota 3700, Kubota, Tokyo, Japan) for 10 min and resuspended in PBS. A 5% stock suspension was prepared. Various BLs were added to the erythrocytes (BL : stock suspension = 1 : 1) and incubated for 4 hr at 37°C. After incubation, the suspensions were centrifuged at 1,000 rpm for 5 min, and the supernatants were collected. Hemolysis was quantified by measuring the absorbance of hemoglobin at a wavelength of 540 nm. Lysis buffer was added to erythrocytes, which was used as the 100% hemolysis sample.

Hindlimb ischemia model. An ischemic hindlimb model was established in five-week-old male ICR mice, as previously reported^{15,32}. Briefly, the animals were anesthetized, and a skin incision was made in the left hindlimb. After ligation of the proximal end of the femoral artery at the level of the inguinal ligament, the distal portion and all side branches were dissected and excised. The right hindlimb was kept intact to control the original blood flow. Measurements of the ischemic (left)/normal (right) limb blood flow ratio were performed for a set time using a laser Doppler blood flow meter (OMEGAFLUO, FLO-C1).



US imaging. Male ICR mice were anesthetized, and injected with an mi-BL solution into the tail vein. Examination of the ischemic hindlimb was performed using an Aplio80 diagnostic US machine (Toshiba Medical Systems, Tokyo, Japan) and a 12-MHz wideband transducer with contrast harmonic imaging at a mechanical index of 0.27.

In vivo miRNA delivery into the skeletal muscle of mice using BLs and US. Ten days after ligation of the femoral artery, a solution of 230 μ L of mi-BLs (200 μ g of BLs (total lipid), 40 μ g of miRNA) was injected into the tail vein, and the site of hindlimb ischemia was immediately exposed to US (frequency, 1 MHz; duty, 50%; burst rate, 2.0 Hz; intensity, 1.0 W/cm²; time, 2 min). A Sonitron 2000 (NEPA GENE, Co., Ltd) was used as a US generator. Blood flow was measured several days after the second injection.

The therapeutic effects of miR-126 delivery using BLs and US. Two or seven days after the second injection, the mice were euthanized, and the thigh muscle in the US-exposed area was collected. The total RNA was extracted with RNAiso Plus. Validation of miR-126 levels was performed as mentioned above. cDNA was synthesized from 1 μ g of the total RNA using Prime Script Reverse Transcriptase (Takara Bio Inc.). Real-time RT-PCR was performed using an ABI PRISM 7000 with SYBR GreenER from Life Technologies (Carlsbad, CA). The primer sequences were previously described⁹. For normalization, validation of 18S ribosomal RNA was performed on cDNA obtained from the same RNA.

In vivo studies. Animal use and relevant experimental procedures were approved by the Tokyo University of Pharmacy and Life Sciences Committee on the Care and Use of Laboratory Animals. All experimental protocols for animal studies were in accordance with the Principle of Laboratory Animal Care at Tokyo University of Pharmacy and Life Sciences.

Statistical analyses. All data are represented as the mean \pm SD ($n = 3-6$). Data were considered significant when $P < 0.05$. A t -test or one-way ANOVA was used to calculate statistical significance.

- Wang, S. *et al.* The endothelial-specific microRNA miR-126 governs vascular integrity and angiogenesis. *Dev. Cell* **15**, 261–271 (2008).
- Fish, J. E. *et al.* miR-126 regulates angiogenic signaling and vascular integrity. *Dev. Cell* **15**, 272–284 (2008).
- van Solingen, C. *et al.* Antagomir-mediated silencing of endothelial cell specific microRNA-126 impairs ischemia-induced angiogenesis. *J. Cell. Mol. Med.* **13**, 1577–1585 (2009).
- Suzuki, R. *et al.* Gene delivery by combination of novel liposomal bubbles with perfluoropropane and ultrasound. *J. Control. Release* **117**, 130–136 (2007).
- Suzuki, R. *et al.* Tumor specific ultrasound enhanced gene transfer *in vivo* with novel liposomal bubbles. *J. Control. Release* **125**, 137–144 (2008).
- Suzuki, R., Takizawa, T., Negishi, Y., Utoguchi, N. & Maruyama, K. Effective gene delivery with novel liposomal bubbles and ultrasonic destruction technology. *Int. J. Pharm.* **354**, 49–55 (2008).
- Negishi, Y. *et al.* Delivery of siRNA into the cytoplasm by liposomal bubbles and ultrasound. *J. Control. Release* **132**, 124–130 (2008).
- Negishi, Y. *et al.* Enhanced laminin-derived peptide AG73-mediated liposomal gene transfer by bubble liposomes and ultrasound. *Mol. Pharm.* **7**, 217–226 (2010).
- Negishi, Y. *et al.* Systemic delivery systems of angiogenic gene by novel bubble liposomes containing cationic lipid and ultrasound exposure. *Mol. Pharm.* **9**, 1834–1840 (2012).
- Endo-Takahashi, Y. *et al.* Efficient siRNA delivery using novel siRNA-loaded Bubble liposomes and ultrasound. *Int. J. Pharm.* **422**, 504–509 (2012).
- Endo-Takahashi, Y. *et al.* pDNA-loaded Bubble liposomes as potential ultrasound imaging and gene delivery agents. *Biomaterials* **34**, 2807–2813 (2013).
- Eliyah, H., Servel, N., Domb, A. J. & Barenholz, Y. Lipoplex-induced hemagglutination: potential involvement in intravenous gene delivery. *Gene Ther.* **9**, 850–858 (2002).
- Kurosaki, T. *et al.* Gamma-polyglutamic acid-coated vectors for effective and safe gene therapy. *J. Control. Release* **142**, 404–410 (2010).
- Taniyama, Y. *et al.* Development of safe and efficient novel nonviral gene transfer using ultrasound: enhancement of transfection efficiency of naked plasmid DNA in skeletal muscle. *Gene Ther.* **9**, 372–380 (2002).
- Negishi, Y. *et al.* Delivery of an angiogenic gene into ischemic muscle by novel bubble liposomes followed by ultrasound exposure. *Pharm. Res.* **28**, 712–719 (2011).
- Christiansen, J. P., French, B. A., Klibanov, A. L., Kaul, S. & Lindner, J. R. Targeted tissue transfection with ultrasound destruction of plasmid-bearing cationic microbubbles. *Ultrasound Med. Biol.* **29**, 1759–1767 (2003).
- Phillips, L. C. *et al.* Focused *in vivo* delivery of plasmid DNA to the porcine vascular wall via intravascular ultrasound destruction of microbubbles. *J. Vasc. Res.* **47**, 270–274 (2010).

- Phillips, L. C., Klibanov, A. L., Wamhoff, B. R. & Hossack, J. A. Targeted gene transfection from microbubbles into vascular smooth muscle cells using focused, ultrasound-mediated delivery. *Ultrasound Med. Biol.* **36**, 1470–1480 (2010).
- Greenleaf, W. J., Bolander, M. E., Sarkar, G., Goldring, M. B. & Greenleaf, J. F. Artificial cavitation nuclei significantly enhance acoustically induced cell transfection. *Ultrasound Med. Biol.* **24**, 587–595 (1998).
- Tachibana, K., Uchida, T., Ogawa, K., Yamashita, N. & Tamura, K. Induction of cell-membrane porosity by ultrasound. *Lancet* **353**, 1409 (1999).
- Enoch, H. G. & Strittmatter, P. Formation and properties of 1000-Å-diameter, single-bilayer phospholipid vesicles. *Proc. Natl. Acad. Sci. U. S. A.* **76**, 145–149 (1979).
- Silvestre, J. S. *et al.* Lactadherin promotes VEGF-dependent neovascularization. *Nat. Med.* **11**, 499–506 (2005).
- Siddiqui, A. J. *et al.* Combination of angiopoietin-1 and vascular endothelial growth factor gene therapy enhances arteriogenesis in the ischemic myocardium. *Biochem. Biophys. Res. Commun.* **310**, 1002–1009 (2003).
- Ye, L. *et al.* Transplantation of nanoparticle transfected skeletal myoblasts overexpressing vascular endothelial growth factor-165 for cardiac repair. *Circulation* **116**, I113–I120 (2007).
- Tavazoie, S. F. *et al.* Endogenous human microRNAs that suppress breast cancer metastasis. *Nature* **451**, 147–152 (2008).
- Sasahira, T. *et al.* Downregulation of miR-126 induces angiogenesis and lymphangiogenesis by activation of VEGF-A in oral cancer. *Br. J. Cancer.* **107**, 700–706 (2012).
- Chen, J. J. & Zhou, S. H. Mesenchymal stem cells overexpressing MiR-126 enhance ischemic angiogenesis via the AKT/ERK-related pathway. *Cardiol. J.* **18**, 675–681 (2011).
- Mochar, P. *et al.* AngiomiR-126 expression and secretion from circulating CD34(+) and CD14(+) PBMCs: role for proangiogenic effects and alterations in type 2 diabetics. *Blood* **121**, 226–236 (2013).
- Negishi, Y. *et al.* AG73-modified Bubble liposomes for targeted ultrasound imaging of tumor neovasculature. *Biomaterials* **34**, 501–507 (2013).
- Owens, C. A. Ultrasound-Enhanced Thrombolysis: EKOS EndoWave Infusion Catheter System. *Semin. Intervent. Radiol.* **25**, 37–41 (2008).
- Haag, P. *et al.* Microbubble-enhanced ultrasound to deliver an antisense oligodeoxynucleotide targeting the human androgen receptor into prostate tumours. *J. Steroid Biochem. Mol. Biol.* **102**, 103–113 (2006).
- Couffignal, T. *et al.* Mouse model of angiogenesis. *Am. J. Pathol.* **152**, 1667–1679 (1998).

Acknowledgments

We are grateful to Prof. Katsuro Tachibana (Department of Anatomy, School of Medicine, Fukuoka University) for technical advice regarding the induction of cavitation with US and to Mr. Yasuhiko Hayakawa and Mr. Kosho Suzuki (NEPA GENE Co., Ltd.) for technical advice regarding US exposure. This study was supported by a Grant for Industrial Technology Research (04A05010) from the New Energy and Industrial Technology Development Organization (NEDO) of Japan, a Grant-in-Aid for Scientific Research (B) (20300179) from the Japan Society for the Promotion of Science, and a Grant-in-Aid for Young Scientists (B) (24790173) from the Japan Society for the Promotion of Science.

Author contributions

Y.E.-T., Y.N. and Y.A. designed the study. Y.E.-T. performed most of the experiments, analyzed data, and wrote the manuscript. A.N. and S.U. contributed to the *in vitro* assay and analyzed data. S.U., K.O. and Y.O. contributed to the analysis of the physical properties of BLs. K.S. and F.M. supported US imaging with key suggestions. N.T. provided technical assistance in the preparation of the hindlimb ischemia model. Y.E.-T., Y.N., R.S. and K.M. contributed to the preparation of BLs. All authors discussed the results and commented on the manuscript.

Additional information

Supplementary information accompanies this paper at <http://www.nature.com/scientificreports>

Competing financial interests: The authors declare no competing financial interests.

How to cite this article: Endo-Takahashi, Y. *et al.* Systemic delivery of miR-126 by miRNA-loaded Bubble liposomes for the treatment of hindlimb ischemia. *Sci. Rep.* **4**, 3883; DOI:10.1038/srep03883 (2014).



This work is licensed under a Creative Commons Attribution-NonCommercial-NoDerivs 3.0 Unported license. To view a copy of this license, visit <http://creativecommons.org/licenses/by-nc-nd/3.0>